© NOV 2025 | IRE Journals | Volume 9 Issue 5 | ISSN: 2456-8880
DOI: https://doi.org/10.64388/IREV9I5-1711756-8734

Synthesis of CeO_2 Nanomaterial Loaded with Pt and Mn Metal Ions as Catalyst for Removal of NOx Compounds Via Low-Temperature REDOX

SULAIMAN TIJJANI NASIRU[1], WEIYUECHANG[2], A. M. USMAN[3], YANG YITAO[4]
[1,3]*Department of Applied Chemistry, Federal University of Technology Babura, P.M.B 2023 Jigawa State, Nigeria.*
[2,4]*Laboratory for optical detection technolopgy for oil and gas, China University of Petroleum, Beijing, China.*

Abstract- ***In this research, a well-defined CeO2 (rod, cube, and polyhedron) were elaborately constructed as the nanocatalysts with predominantly exposed facets of {110}, {100}, and {111}, respectively. TheCeO2nanocube catalyst supported with metals ion (Mn and Pt) was successfully synthesized by gas bubbling-assisted membrane reduction (GBMR) method. Activity test results show that all the synthesized catalysts are good, but PtMn-CeO2 catalyst has the best soot burning activity (T50 = 367 oC). The PtMn-CeO2 catalyst has the best catalytic activity. The synergy between Pt and Co can effectively increase the number of surface oxygen vacancies and promote surface active oxygen generation. Thereby accelerating the adsorption and activation of reactant molecules (O2 and NO) and increasing the mobility of lattice oxygen.Through various characterizations (SEM, BET and H2-TPR), the effect of CeO2 catalyst on crystal plane was systematically studied. The study showed that the catalytic activity of CeO2NOx removal catalyst which mainly exposed {110} crystal plane and its excellent low-temperature oxidation-reduction performance was found to be more promising in terms of totalNOx particles removal.The research discovered that using gas film assisted reduction method; platinum and manganese nanoparticles were uniformly dispersed and loaded onto cerium dioxide carriers. Through SEM characterization, it was evident that Pt/Mn CeO2 and other catalysts were successfully prepared and the morphology of the loaded catalysts remained intact. Cerium dioxide demonstrated some catalytic activities which were further enhanced by the addition of Pt and Mn nanoparticles. Notably, when Pt and Mn nanoparticles were loaded simultaneously, the T50 of Pt/Mn-CeO2 decreased to 367°C under loose contact conditions.***

Key Words : ***Ceo2-Based Catalyst; Nanomaterial; Oxidation; Synergy Effect; Active Oxygen Species; Nox-Compound.***

I. INTRODUCTION

Nitrogen and Oxygen compounds (NO_x) emitted by diesel vehicle exhaust are among the main environmental pollutants[1]. These compounds are easy to produce acid rain, photochemical smog and other environmental problems. It is important to control the emission of nitrogen and oxygen compounds in diesel vehicle exhaust[1]. In diesel vehicle tail gas post-treatment technology, catalysts coated in diesel particle catcher are generally used to oxidize NO to become NO_2, and then the strong oxidation performance of NO_2 is used to oxidize and eliminate soot particles[2].According to the "2016-2019 National Ecological Environment Statistical Bulletin" in China, NO_x emissions in the national exhaust emissions reached 12.339 million tons, of which 6.556 million tons were emitted by mobile sources, accounting for more than 50%; PM emissions reached 10.885 million tons, of which 74,000 tons were emitted by mobile sources[2]. In mobile sources, cars emit more than 90% of pollutants[3]. As of the end of March 2022, the number of motor vehicles in the country reached 402 million, including 307 million cars, with the popularity of automobiles, the exhaust gas generated during automobile driving has become one of the important sources of air pollution[2], and the urgency of motor vehicle pollution prevention and control has become increasingly prominent. In the face of the current grim situation of environmental pollution, the report of the 20th National Congress clearly pointed out that it is necessary to accelerate the green transformation of development mode and further promote the prevention and control of environmental pollution[3]. As a result, the development of more sophisticated catalytic technologies has become necessary for treatment of automotive exhaust and to comply with national regulations on automotive

© NOV 2025 | IRE Journals | Volume 9 Issue 5 | ISSN: 2456-8880
DOI: https://doi.org/10.64388/IREV9I5-1711756-8734

exhaust control[4]. Reducing NOx emissions from vehicle exhaust is a crucial and formidable objective. To address this challenge, this study was conducted to design catalysts with different morphologies using cerium dioxide supports. The study also involved the addition of platinum and manganese to enhance the catalyst's intrinsic catalytic activity and investigate their role in NOx combustion catalysis. There are two main ways to improve the activity of NOx removal: one is to improve the contact site between the NOx compounds and catalyst; the second is to improve the redox performance of the catalyst[4]. Transition metal-based nanomaterials have attracted more and more attention due to their superior redox performance and their cheap and easy-to-obtain characteristics[5]. Modifying transition metal-based nanomaterials to improve their catalytic performance is expected to replace precious metal catalysts in the future. In this paper, cerium-based nanomaterial is selected as the research objects, and the catalytic activity of the materials is improved from two directions: Firstly, the CeO_2 (rod, cube, and polyhedron) were elaborately constructed the nanocatalysts with predominantly exposed facets of {110}, {100}, and {111}, respectively. The order catalytic activity of the three catalysts is CeO_2-R > CeO_2-O > CeO_2-C, CeO_2-R catalyst has an activity index value T_{50} of 413 ºC, and has good stability and high CO_2 selectivity. Through various characterizations, the effect of CeO_2 catalyst on NOx compounds removal crystal plane was systematically studied.

II. METHODOLOGY

2.1 Preparation of catalysts

CeO_2nano-rods (CeO_2−R) were synthesized by a hydrothermal method. Generally, 1.96 g of $Ce(NO_3)_3 \cdot 6H_2O$ and 16.88g of NaOH were dissolved in 40 and 30 mL of deionized water (DI water), respectively. After cooling naturally, the NaOH solution was added dropwise into a cerium nitrate solution to form a mixture. After stirring for 0.5 h, the resulting slurry was moved into a 100mL volume autoclave. Hydrothermal treatment was conducted at 373 K for duration of 24 h. The obtained precipitate was first wash or with both DI water and ethanol, collected by centrifugation, and finally dried at 353 K for duration of 8 h[6]. The final products were acquired by the process of calcination, will be carried out by exposing the sample to an air atmosphere at a temperature of 673 K for duration of 4 hours.

CeO_2nano-octahedra (CeO_2−O) were prepared by following a previously reported method[6]. Typically, 0.858 g of $Ce(NO_3)_3 \cdot 6H_2O$ and 0.0075 g of Na_3PO_4 were dissolved in 10 and 70 mL of deionized water, respectively. After mixing and stirring, the resulting solution was moved into a 100 mL autoclave. Hydrothermal treatment was conducted at 443 K for duration of 10 h. The obtained precipitate was first wash or clean with both DI water and ethanol, collected by centrifugation, and finally dried at 353 K for duration of 8 h. The final products were acquired by calcination in an air atmosphere at 673 K for duration of 4 h[7].

CeO_2nano-cubes (CeO_2−C) were synthesized by a hydrothermal process[7].Generally, 1.96 g of $Ce(NO_3)_3 \cdot 6H_2O$ and 16.88 g of NaOH were dissolved in 40 and 30mL of deionized water (DI water), subsequently. After cooling naturally, a NaOH solution was added dropwise into a $Ce(NO_3)_3$ solution to form a mixture. After stirring for 0.5 h, the resulting slurry was moved into a 100mL volume autoclave. Hydrothermal treatment was conducted at 453 K for duration of 24 h. The obtained precipitate was first wash or clean with both DI water and ethanol, collected by centrifugation, and finally dried at 353 K for duration of 8 h. The final products were acquired by the process of calcination in an air atmosphere at 673 K for duration of 4 h.Pt and other metals were supported by GBMR (gas bubbling-assisted membrane reduction-precipitation) technique was utilized to facilitate reduction and precipitation processes during the experiment[7]. However a protective agent in the form of polyvinyl pyrrolidone (PVP) was employed during the experiment was added to control the particle size. Firstly, $PtCl_6^-$ ions are adsorbed and anchored on surface OH_2^+ groups on the CeO_2 support formed because of the pH value of the solution is lower than the isoelectric point of the CeO_2 support. Simultaneously, a hybrid between $PtCl_6^-$ ions and capping ligands of the poly(N-vinyl-2-pyrrolidone) (PVP) might form. When $NaBH_4$ was highly homogeneously dispersed into the holes (d=40 nm) the tubular reactor with a ceramic membrane facilitated the reduction of $PtCl_6$- leading to the formation of Au nucleus. This process was carried out with adequate protection, which restricted the growth of crystal nucleus on the surface of CeO_2 supports. The H_2 gas bubbling, which was maintained at a steady pace, played a crucial role in promoting mass transfer, reducing dead space, and enhancing

© NOV 2025 | IRE Journals | Volume 9 Issue 5 | ISSN: 2456-8880
DOI: https://doi.org/10.64388/IREV9I5-1711756-8734

the even distribution of Au nanoparticles on the CeO_2 carrier The appropriate adjustment of reaction conditions, including the PVP concentration and the whole size of ceramic membrane, provides an effective way to control the dispersion and size of Au nanoparticles. The actual content of Au in catalysts was determined by inductively coupled plasma atomic emission spectrometry (ICP-AES)[8].

III. CHARACTERISATION

3.1 BET specific surface area analysis

The N_2 physical adsorption method was used to determine the specific surface area of the catalyst. The specific surface analysis of the samples in this paper was performed using the Micromeritics ASAP 2020 fully automated specific surface analyzer[8].

3.4 Scanning electron microscopy (SEM)

Shape and microstructure of the catalyst are directly observed using the field emission environment scanning electron microscope (FEI Quanta 200F) produced by FEI in the United States. Technical indicators: accelerating voltage is 5 kV; the resolution is 1.2 nm. Magnification 25-200 K, scanning mode is high vacuum mode, low vacuum mode, ring scanning mode. X-ray energy loss spectroscopy (EDX) can simultaneously analyze the surface and composition of solid materials[9].

3.5 H_2-programmed temperature reduction (H_2-TPR)

Catalysts with metal oxide supported noble metal nanoparticles have a certain reduction temperature and strength, which represents the oxidation performance of the catalyst. H_2-TPR is one of the effective methods to study oxidation-catalytic interactions between metal ions or between precious metal particles and supports[10].

IV. NOx REMOVAL EXPERIMENT

NO-TPO uses the Quantachrome autosorb-1 quadrupole mass spectrometer to detect the concentration of NO_2 at the reaction outlet on the line. Since NO plays an important role in the catalytic soot combustion, NO is catalytically oxidized to NO_2, which is an important intermediate product in soot oxidation. Therefore, the catalytic oxidation capacity of the catalyst to NO is related to the performance of the catalyst.In this paper, NO-TPO experiment was performed on a homemade fixed-bed tubular quartz reactor. Pretreat 100 mg of catalyst at 200 °C for 0.5 h under N_2 atmosphere. Then, at a total flow rate of 50 mL min^{-1}, composed of 5 v% O_2, 0.2 v% NO and N_2 as equilibrium gases, the catalyst is heated from 150 °C to 500 °C at a heating rate of 2 °C min^{-1}[10],[11].

In this research, the performance of the synthesized catalysts was tested on a self-made atmospheric pressure micro-fixed-bed reaction device. The NOx particles used in the experiment were Printex U commercial carbon particles produced by Degussa. The 0.1 g catalyst and 0.01 g NOx particles were mixed evenly with a sample spoon, and the contact mode was loose contact, which was closest to the actual working conditions[12]. The evenly mixed sample was loaded into an atmospheric fixed quartz tube with a pipe diameter of 6 mm, fixed with quartz wool at both ends, and the quartz tube was placed in the constant temperature section of the tube furnace, the heating rate was 2°C min^{-1}, and the reaction atmosphere was 2000 ppm NO, 5 v% O_2 and Ar with a gas flow rate of 50mL min^{-1}. Also the reaction outlet gas is analyzed qualitatively and quantitatively by GC 9890B gas chromatography produced by Shanghai Linghua Instrument Co., Ltd. Porapak N column was used to separate CO and CO_2 produced by soot combustion, the product concentration is quantitatively detected by FID hydrogen flame ion detector[13].

V. RESULTS AND DISCUSSIONS

The results of the experiments as well as the characterization of the catalysts prepared are presented and also explained under the below highlighted headings.

5.1 NO-TPO measurement

In order to explore the catalytic potential of CeO_2 with catalysts having three different morphologies for NO oxidation, NO-TPO tests were conducted using online FT-IR spectroscopy.

© NOV 2025 | IRE Journals | Volume 9 Issue 5 | ISSN: 2456-8880
DOI: https://doi.org/10.64388/IREV9I5-1711756-8734

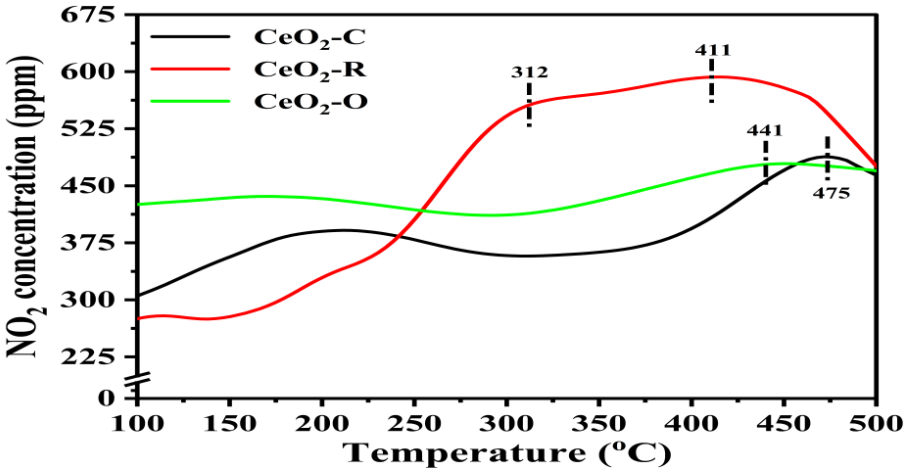

Figure 1: Plot ofNO_2 profiles of NO oxidation with three different CeO2 morphologies with increasing temperature

As shown in figure 1, it was observed that the concentration of NO_2 played a critical role in the catalytic mechanism for soot oxidation. The temperature corresponding to peak concentration of NO_2 can be seeing as an important parameter to evaluate oxidation ability for catalysts. However, CeO_2-R at peak NO2 concentration occurs at lower temperature (411 °C) compared to CeO_2-C and CeO_2-O catalysts. This indicates that CeO_2-R catalyst has excellent ability to activate NO molecule than the others. In addition, it can also be seeing that the activity of CeO_2 catalysts for NO oxidation is dependent on the exposed crystal facets of CeO_2[14].

VI. NO OXIDATION

The more robust oxidizing properties of NO_2 in comparison to NO and O_2 are widely acknowledged. The oxidation process of NO to NO_2 is a crucial stage in the catalytic oxidation of soot in vehicle emissions consisting of NO and O_2. This mechanism is commonly referred to as the NO_2-assisted catalytic combustion process for diesel soot particles[15]. Although diesel exhausts predominantly comprises NO_x gas in the form of NO, with minimal presence of NO_2. Consequently, it is crucial to enhance the activation capacity of catalysts for gaseous reactants such as O_2 and NO. Figure 2 illustrates the results of NO oxidation experiments which were conducted to determine the concentration of NO_2 that resulted from oxidation of NO across all the prepared catalysts with nanocube structure. The catalytic activity of pure CeO_2 catalyst for NO oxidation was found to be poor with only 20% conversion at 300-500°C. On the other hand, PtMn/CeO_2-C catalyst demonstrates superior activity for oxidation of NO to NO_2, at a peak temperature of about 403 °C. This is accompanied by an increase in the NO_2 concentration within the same temperature range[15]. This observation suggests that PtMn/CeO_2-C catalyst outperformed the other catalysts in terms of NO oxidation activity. Furthermore, the concentration of NO_2 resulting from the catalysts remains constant as the temperature increases until it reaches a thermodynamic equilibrium point which can be expressed using the equation ($NO + 1/2O_2 \leftrightarrow NO_2$).

After this point, the concentration of NO_2 decreases with further temperature increase and it conforms to the thermodynamic profile. This indicates that the NO_2 concentration is not affected solely by temperature but rather by the equilibrium established by the reaction[16].

© NOV 2025 | IRE Journals | Volume 9 Issue 5 | ISSN: 2456-8880
DOI: https://doi.org/10.64388/IREV9I5-1711756-8734

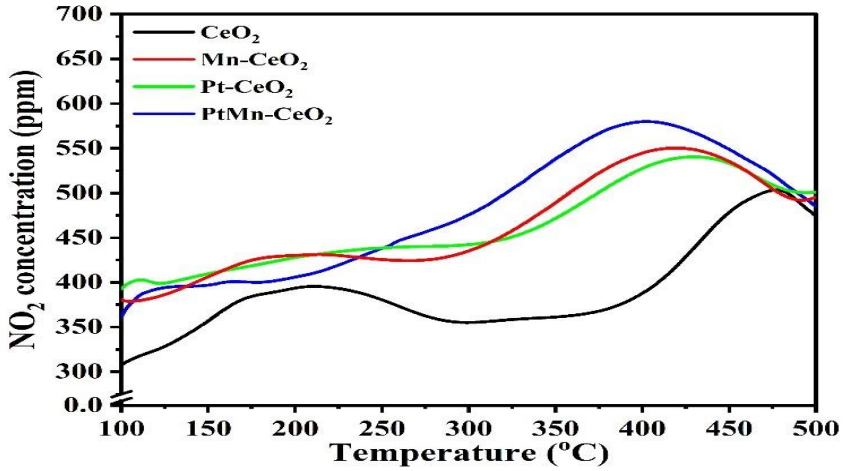

Figure 2: The NO-TPO profiles over CeO_2, Mn-CeO_2, Pt-CeO_2 and PtMn-CeO_2.

VII. THE BET ANALYSIS

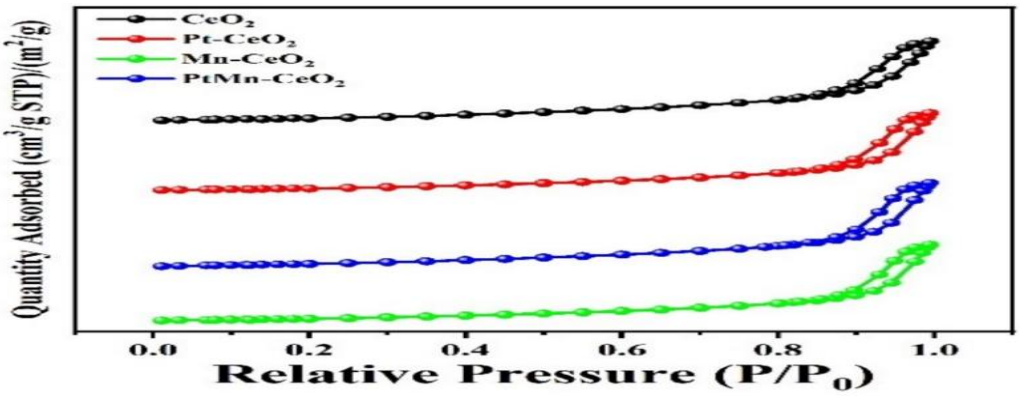

Figure 3: Nitrogen adsorption−desorption isotherms of as-prepared catalysts.

Results from the nitrogen adsorption-desorption isotherms for the four catalysts (i.e. CeO_2, Mn-CeO_2, Pt-CeO_2 and PtMn-CeO_2), are presented in figure 3. In terms of adsorption and desorption behavior, the isotherms for the freshly prepared catalysts exhibit a standard type IV pattern similar to that of IUPAC classification[17]. The shapes of the adsorption-desorption isotherms are also comparable to one another. In addition, based on the data presented in table 4.2, PtMn-CeO_2 boasts the greatest surface area, whereas Mn-CeO_2 and Pt-CeO_2 exhibit nearly identical surface areas which are somewhat lower than that of PtMn-CeO_2. The pattern of total pore volume and pore size aligns with the order of surface area. It should be noted that the surface areas of these catalysts are below 30 m^2/g, which is lower than other particle catalysts[18]. It is worth mentioning that the application of a CeO_2 coating creates additional voids within the particles and it somewhat increases the S_{BET} of PtMn-CeO_2. However, the crucial factor for NO catalytic oxidation is the number of contact points between the catalyst and NO rather than the S_{BET}[19].

Table 1:Values obtained for BET surface areas (S_{BET}), pore volume (V_p), pore diameter (D_p) and crystal size is all as-prepared catalysts.

	S_{BET}[a]	V_p[b]	D_p[c]	Crystal size [d]
Catalysts	(m^2/g)	(cm^3/g)	(nm)	(nm)
CeO_2-C	18.2	0.177	13.6	40.6
CeO_2-R	98.8	0.472	15.8	9.5
CeO_2-O	26.1	0.009	8.3	17.8

© NOV 2025 | IRE Journals | Volume 9 Issue 5 | ISSN: 2456-8880
DOI: https://doi.org/10.64388/IREV9I5-1711756-8734

VIII. MORPHOLOGICAL STUDY

In this study, the catalysts prepared were examined using scanning electron microscopy (SEM) in order to check their morphological behaviors. Basically, hydrothermal method was used for synthesizing CeO_2 catalyst and three different morphologies (i.e. CeO_2-C, CeO_2-R and CeO_2-O) were obtained. In addition, agglomeration of the catalyst with three morphologies also occurred as shown in figures 5A, D and G. Further, transmission electron microscopy (TEM) was also employed in order to probe the crystal growth and the structures of the all as-prepared catalysts with different morphology[21]. As shown in figure 5B, the nanocube morphology of CeO_2-C has approximately 10-30 nm diameters. However, CeO_2-R catalyst shows a uniform diameter of 10 nm with its length in the range of 40-100 nm as shown figure 5E. An interplane spacing of 0.19 and 0.31 nm was attributed to the (110) and (111) planes as observed in figure 5F. The polyhedron shape of CeO_2-O catalyst is also synthesized with a uniform particle size of 10-30 nm (Figure 4H [22].

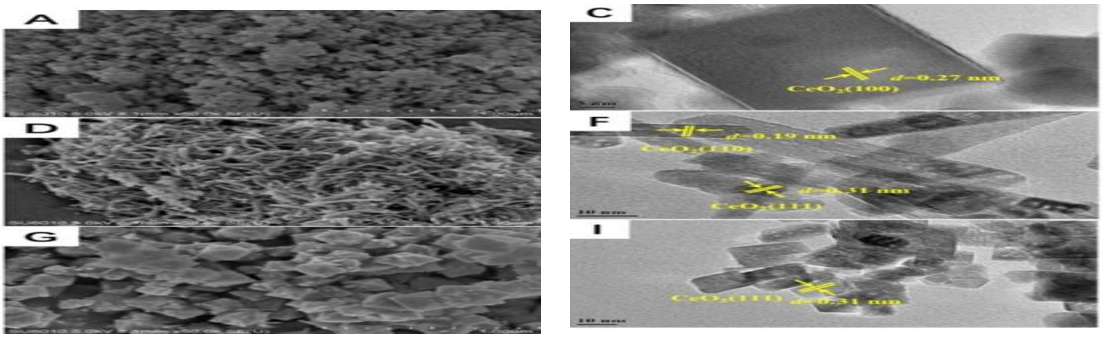

Figure 5: SEM images (A, D and G) and HRTEM (C, F and I) images of CeO_2-C, CeO_2-R and CeO_2-O respectively.

IX. MEASUREMENTS OF SPECIFIC SURFACE AREA USING N_2 ADSORPTION-DESORPTION.

The specific surface area (S_{BET}) and pore structure of all catalysts were deduced using N_2 adsorption-desorption method at -196ºC. The results obtained are presented in figure 6 below. The representative N_2 adsorption-desorption isothermal and size distribution curves of all as-prepared catalysts can be vividly seeing. As shown in figure 6A, all the catalysts exhibit a small H4 hysteresis loop in the P/P_0 range of 0.8 to 1.0[23].

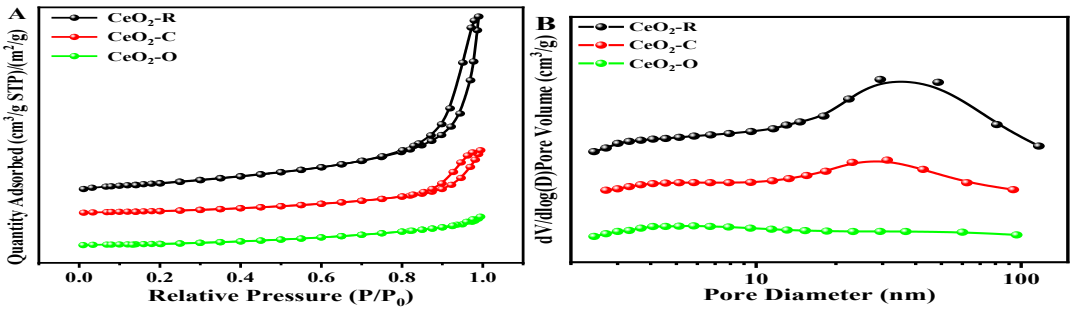

Figure 6: (a) Nitrogen adsorption-desorption isotherms. (b) Pore size distribution curves of CeO_2 catalysts with the three morphologies.

The S_{BET}, average mesopore size (D_p) and total pore volume (V_p) values of all as-prepared catalysts are listed in Table 1. Among all as-prepared catalysts, the CeO_2-R catalyst has the largest specific surface area (98.8 m^2 g^{-1}). The pore size distribution results of all as-prepared catalyst are also shown in figure 6B. The pore size of CeO_2 catalysts are within the range of 10-100 nm. This indicates the presence of porous structure in all as-prepared catalysts[23]. The formation of this porous structure can be attributed to the nanoparticles being stacked on top of one another . Surface area were obtained by BET method; Pore volume were obtained by BET method; Pore

© NOV 2025 | IRE Journals | Volume 9 Issue 5 | ISSN: 2456-8880
DOI: https://doi.org/10.64388/IREV9I5-1711756-8734

diameter were calculated via the BJH method according to the N_2 desorption isotherm.

X. REDOX PROPERTIES.

The redox properties of all as-prepared catalysts were measured with the aid of H_2-TPR experiments. As shown in Figure 7, the CeO_2 catalysts with three different morphologies show different reduction temperature. The reduction of ceria surface oxygen occurs with the maxima at 715, 553 and 495°C for CeO_2-C, CeO_2-R and CeO_2-O respectively.

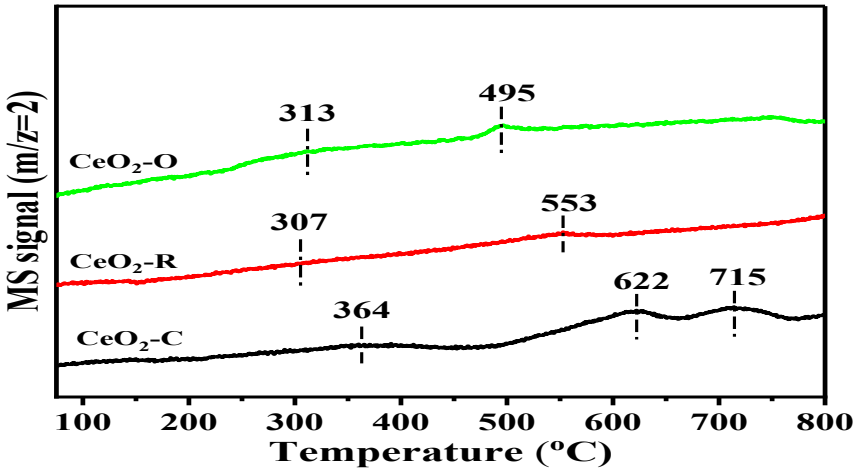

Figure 7: Plot ofH_2-TPR profiles with three different morphologies for CeO_2 catalyst.

Reduction temperature within the range of 307 to 364°C, can be attributed to reduction of surface oxygen in CeO_2. Generally, the process of reducing bulk oxygen over CeO_2 occurs within the temperature range of about 495 to 715 °C [34]. However, CeO_2-R catalyst shows strongest reduction property at relatively low temperature (307 °C) in comparison with CeO_2-C and CeO_2-O catalysts. This indicates that CeO_2-R with exposed {110} facet has better redox property than those with {100} and {111} facet[24].

XI. CONCLUSION

The results from this study using H_2-TPR and NO-TPO experiments show that CeO_2-R catalyst has excellent oxidation property which enables it to rapidly convert NO to NO_2 thereby enhancing oxidation. Based on findings in this study, the order of crystal facet-dependent activity for NOx oxidation/removal is as follows: CeO_2{110} > CeO_2{100} > CeO_2 {111}. This research has wide practical applications and it highlights a new strategy for fabrication of efficient CeO_2-based catalysts with optimized surface facets which can be used to monitor diesel soot particles or other pollutants which represent future nanomaterial for soot removal. Activity test results show that all the synthesized catalysts are very good, but PtMn-CeO_2 catalyst has the best NOx removal activity (T_{50} = 367 °C).

REFERENCES

[1] Matti Maricq, M.(2007) Chemical Characterization of Particulate Emissions from Diesel Engines: A Review. Journal of Aerosol Science., 38 (11), 1079–1118.

[2] Moorthi, M.; Murugesan, A.; Alagumalai, A.(2022)“Effect of Nanoparticles on DI-CI Engine Characteristics Fueled with Biodiesel–Diesel Blends” A Critical Review. J Therm Anal Calorim., 147 (17), 9163–9179.

[3] Stanmore, B. R.; Brilhac, J. F.; Gilot, P. The Oxidation of Soot: A Review of Experiments, Mechanisms and Models. Carbon. 2001, 39 (15), 2247–2268.

[4] Fino, D.; Russo, N.; Saracco, G.; Specchia, V. Removal of NOx and Diesel Soot over Catalytic Traps Based on Spinel-Type Oxides. Powder Technology. 2008, 180 (1), 74–78.

[5] Wu, Q.; Xiong, J.; Mei, X.; Zhang, Y.; Wei, Y.; Zhao, Z.; Liu, J.; Li, J. Efficient Catalysts of La2O3 Nanorod-Supported Pt Nanoparticles for Soot Oxidation: The Role of La2O3 - {110}

Facets. Industrial Engineering Chemistry Research. 2019, 58 (17), 7074–7084.

[6] Lee, J. H.; Jo, D. Y.; Choung, J. W.; Kim, C. H.; Ham, H. C.; Lee, K.-Y. Roles of noble metals (M = Ag, Au, Pd, Pt and Rh) on CeO2 in enhancing activity toward soot oxidation: Active oxygen species and DFT calculations. Journal of Hazardous Materials.2021, 403, 124085.

[7] Machida, M.; Murata, Y.; Kishikawa, K.; Zhang, D.; Ikeue, K. On the Reasons for High Activity of CeO2 Catalyst for Soot Oxidation.Chemistry Materials. 2008, 20 (13), 4489-4494.

[8] Ashikaga, R.; Murata, K.; Ito, T.; Yamamoto, Y.; Arai, S.; Satsuma, A. Tuning the oxygen release properties of CeO2-based catalysts by metal–support interactions for improved gasoline soot combustion. Catalysis Science & Technology. 2020, 10 (21), 7177-7185.

[9] Kim, G. J.; Kwon, D. W.; Hong, S. C. Effect of Pt Particle Size and Valence State on the Performance of Pt/TiO2 Catalysts for CO Oxidation at Room Temperature. Journal of Physical Chemistry C. 2016, 120 (32), 17996–18004.

[10] Xiong, M.; Gao, Z.; Qin, Y. Spillover in Heterogeneous Catalysis: New Insights and Opportunities. ACS Catalyst. 2021, 11 (5), 3159–3172.

[11] Yao, P.; Huang, Y.; Jiao, Y.; Xu, H.; Wang, J.; Chen, Y. Soot Oxidation over Pt-Loaded CeO2-ZrO2 Catalysts under Gasoline Exhaust Conditions: Soot-Catalyst Contact Efficiency and Pt Chemical State. Fuel.2023, 334, 126782.

[12] Lee, S.; Lee, H.; Song, C.; Park, J. Experimental Study on Fundamental Effect of H2 for Catalytic Soot Oxidation with Pt/CeO2 Using a Flow Reactor System. Journal of the Energy Institute. 2019, 92 (5), 1419–1427.

[13] Wei, Y.; Wu, Q.; Xiong, J.; Li, J.; Liu, J.; Zhao, Z.; Hao, S. Efficient catalysts of supported PtPd nanoparticles on 3D ordered macroporous TiO2 for soot combustion: Synergic effect of Pt-Pd binary components. Catal. Today 2019, 327, 143-153.

[14] Wei, Y.; Jiao, J.; Zhang, X.; Jin, B.; Zhao, Z.; Xiong, J.; Li, Y.; Liu, J.; Li, J. Catalysts of Self-Assembled Pt@CeO2−δ-Rich Core–Shell Nanoparticles on 3D Ordered Macroporous Ce1−xZrxO2 for Soot Oxidation: Nanostructure-Dependent Catalytic Activity. Nanoscale 2017, 9 (13), 4558–4571.

[15] Lee, J. H.; Lee, S. H.; Choung, J. W.; Kim, C. H.; Lee, K.-Y. Ag-incorporated macroporous CeO2 catalysts for soot oxidation: Effects of Ag amount on the generation of active oxygen species. Applied Catalysis B: Environmental. 2019, 246, 356-366.

[16] Andana, T.; Piumetti, M.; Bensaid, S.; Veyre, L.; Thieuleux, C.; Russo, N.; Fino, D.; Quadrelli, E. A.; Pirone, R. CuO Nanoparticles Supported by Ceria for NOx-Assisted Soot Oxidation: Insight into Catalytic Activity and Sintering. Applied Catalysis B: Environmental 2017, 216, 41–58.

[17] Wagloehner, S.; Baer, J. N.; Kureti, S. Structure–activity relation of iron oxide catalysts in soot oxidation. Applied Catalysis B: Environmental 2014, 147, 1000-1008.

[18] Legutko, P.; Jakubek, T.; Kaspera, W.; Stelmachowski, P.; Sojka, Z.; Kotarba, A. Soot oxidation over K-doped manganese and iron spinels — How potassium precursor nature and doping level change the catalyst activity. Catal.Commun. 2014, 43, 34-37.

[19] Zhang, Y.; Zou, X. The Catalytic Activities and Thermal Stabilities of Li/Na/K Carbonates for Diesel Soot Oxidation. Catalysis Communications 2007, 8 (5), 760–764.

[20] Atribak, I.; Bueno-López, A.; García-García, A. Combined Removal of Diesel Soot Particulates and NOx over CeO2–ZrO2 Mixed Oxides. Journal of Catalysis 2008, 259 (1), 123–132.

[21] Zhang, Y.; Zhang, P.; Xiong, J.; Wei, Y.; Jiang, N.; Li, Y.; Chi, H.; Zhao, Z.; Liu, J.; Jiao, J. Synergistic Effect of Binary Co and Ni Cations in Hydrotalcite-Derived Co2-xNixAlO Catalysts for Promoting Soot Combustion. Fuel 2022, 320, 123888.

[22] Shang, Z.; Sun, M.; Chang, S.; Che, X.; Cao, X.; Wang, L.; Guo, Y.; Zhan, W.; Guo, Y.; Lu, G. Activity and Stability of Co3O4-Based Catalysts for Soot Oxidation: The Enhanced Effect of Bi2O3 on Activation and Transfer of Oxygen. Applied Catalysis B: Environmental 2017, 209, 33–44.

[23] Zhai, G.; Wang, J.; Chen, Z.; An, W.; Men, Y. Boosting Soot Combustion Efficiency of Co3O4 Nanocrystals via Tailoring Crystal Facets. Chemical Engineering Journal 2018, 337, 488–498.

[24] Xie, X.; Li, Y.; Liu, Z.-Q.; Haruta, M.; Shen, W. Low-temperature oxidation of CO catalysed by Co3O4 nanorods. Nature 2009, 458 (7239), 746-749.

[25] Li, Y.; Li, K.; Wang, Y.; Zhou, K.; Zhao, M.; Hu, M.; Liu, Y.-Q.; Qin, L.; Cui, B. Fe-Doped Porous Co3O4 Nanosheets with Highly Efficient Catalytic Performance for Soot Oxidation. Chemical Engineering Journal 2022, 431, 133248.